Supporting information

Sequence defined oligomer as a modular platform for selective sub-picomolar detection of Hg^{2+} and removal of the same

Anna Jose, Pandurangan Nanjan, Mintu Porel*

Discipline of Chemistry, Indian Institute of Technology Palakkad, Kerala-678577, India

Table of Contents

1. Materials and methods

All the chemicals were purchased from Sigma Aldrich, Alfa Aesar and Spectrochem. ^{1}H NMR spectra were recorded on INOVA-400 spectrometers. ^{1}H NMR data were analysed by MestReNova (version 8.1.1). ^{1}H NMR chemical shifts are reported in units of ppm relative to tetramethylsilane. ^{1}H NMR data are presented in the following order: chemical shift, peak multiplicity (s = singlet, d = doublet, t = triplet, m = multiplet, dd = doublet of doublet, dt = doublet of triplet), coupling constant, proton number. LC-MS experiments were carried out on a Shimadzu LC-MS-8045 with a Sprite TARGA C18 column (40 × 2.1 mm, 5 µm) monitoring at 210 and 254 nm with positive mode for mass detection. Solvents for LC-MS were water with 0.1% acetic acid (solvent A) and acetonitrile with 0.1% acetic acid (solvent B). Compounds were eluted at a flow rate of 0.7 mL/min with a gradient of 5% solvent B for 2 min, followed by a linear gradient from 5% to 40% solvent B over 4 min, followed by changing the solvent B from 40% to 60% for 10 min and finally, it was brought down to 5% solvent B in 2 min and then continued till for 2 min before the method stopped. Column was washed with 50% Solvent B followed by 95% Solvent B always before sample injection. Mass spectrometry was performed on a Shimadzu mass spectrometer using positive ionization and a linear detector. Purity analysis was carried out using Shimadzu HPLC-20AP instrument. The same solvent system such as 0.1% acetic acid (solvent A) and acetonitrile with 0.1% acetic acid (solvent B) and the same solvent gradient as LC-MS were used for the HPLC analysis. Fluorescence was recorded on Perkin Elmer FL 6500. All fluorescence spectra were recorded at 25^{0}C with an excitation wavelength of 278nm and excitation and emission slit width of 5nm. SEM images were taken using Carl Zeiss - Gemini SEM 300 with 2000000 X magnification and a resolution of 0.8nm at 15 kV; 1.3 nm at 1 kV. The quantitative analysis of mercury was done using inductively coupled plasma mass spectrometer (ICP-MS) instrument (Thermo Fisher iCAP RQ ICP-MS).

2. Synthesis of monomers

The monomers were synthesized through two consecutive reactions. Details of the reactions are given below.

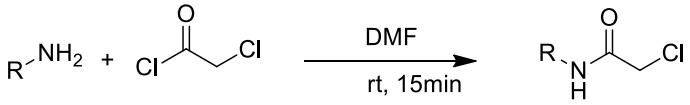

Scheme S1. Synthesis of chloro-terminal amides

Chloro-terminal amides were synthesized by the reaction of substituted amines (1 mmol) and chloroacetyl chloride (1.5 mmol) in DMF (5 mL). The reaction was carried out at 0^{o}C during the addition of chloroacetyl chloride and then brought to room temperature. After completion of the reaction (monitored by TLC), the excess chloroacetyl chloride was quenched by the addition of sodium bicarbonate ($NaHCO_3$). The reaction mixture was extracted in 1:1 ethyl acetate/water. Ethyl acetate layer was dried over anhydrous Na_2SO_4 and the product was isolated from ethylacetate layer. The solvent was removed under reduced pressure and the products were obtained with high purity (>95%).

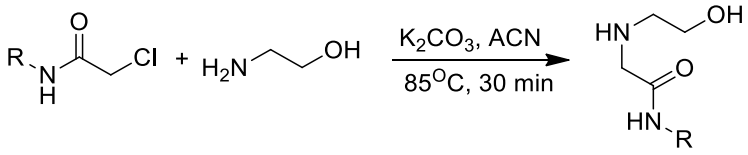

Scheme S2. Synthesis of amine hydroxy monomer

The monomers were prepared by the reaction of chloro-terminal amides (1 mmol) and ethanolamine (5 mmol) in acetonitrile (5 mL) in presence of potassium carbonate (K_2CO_3, 10 mmol) as base. The reaction mixture was refluxed for 30 min. Thereafter, the reaction mixture was extracted in1:1ethylacetate/water mixture. Ethyl acetate layer was dried over anhydrous Na_2SO_4. The solvent was removed under reduced pressure and product was obtained at good yield (90-95%) with >95% purity. Monomers were directly used for polymerization reaction without further purification.

3. Synthesised monomers and their characterisation by ^{1}H- NMR

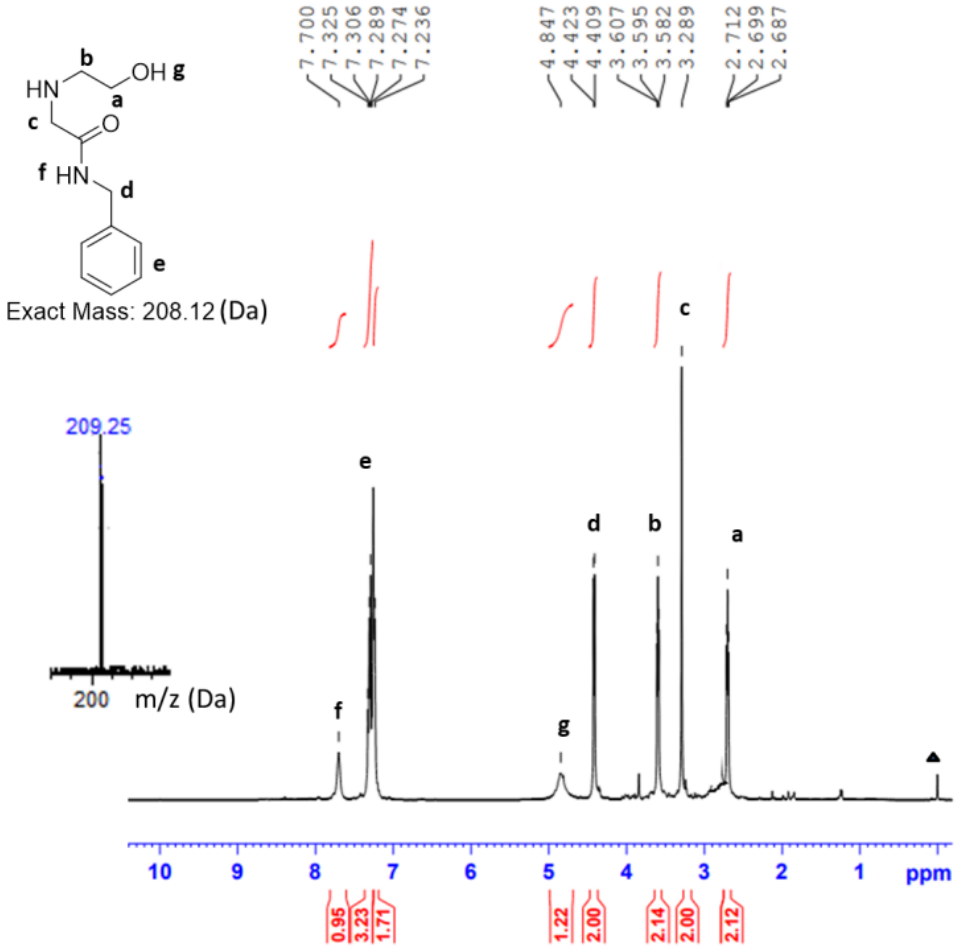

Fig S1. ^{1}H NMR spectra (400 MHz, $CDCl_3$) of benzyl ethanolamine monomer: δ (ppm) 2.68 (t, J = 4.8 Hz, 2H), 3.28 (s, 2H), 3.58 (t, J = 4.8 Hz, 2H), 4.40 (d, J = 5.6, 2H), 7.23-7.32 (m, 5H); LC-MS calculated $[M+H]^+$: 209.12 Da, observed: 209.25 Da. "▲" represents the residual proton of internal standard tetramethylsilane.

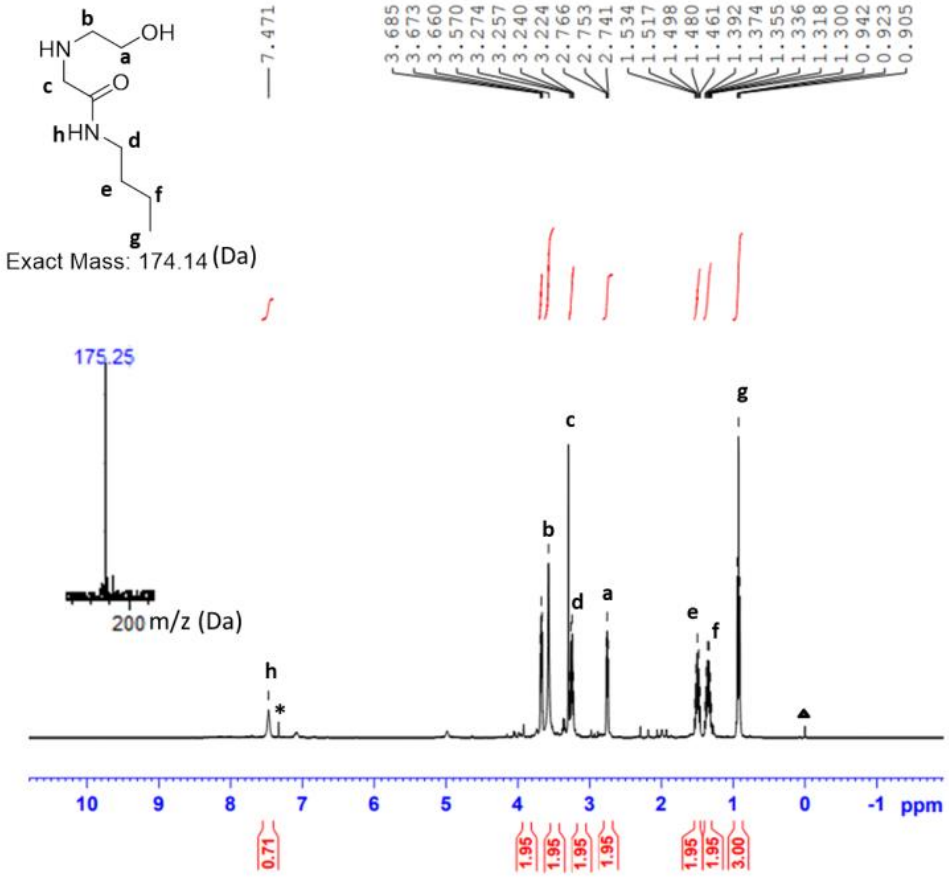

Fig S2. ^{1}H NMR spectra (400 MHz, $CDCl_3$) of butyl ethanolamine monomer: δ (ppm) 0.90 (t, J = 7.6 Hz, 3H), 1.30 (m, 2H), 1.35 (m, 2H), 2.74 (t, J = 4.8 Hz, 2H), 3.22 (t, J = 6.8 Hz, 2H), 3.57 (s, 2H), 3.66 (t, J = 4.8 Hz, 2H); LC-MS calculated $[M+H]^+$: 175.14 Da, observed: 175.25 Da. "*" represents the residual proton signal of $CDCl_3$ and "▲" represents the residual proton of internal standard tetramethylsilane.

4. Synthesis of sensors and their starting materials

4.1 Synthesis of sensor 1

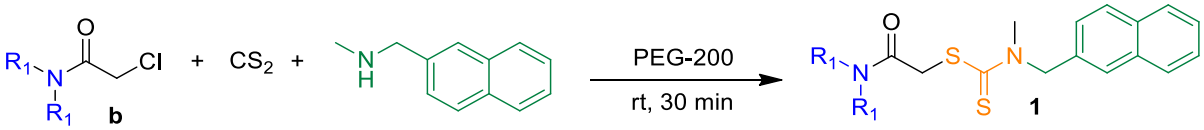

Scheme S3. Synthesis of sensor **1**

Chloro terminal amide (**b**, 1 mmol), N-methyl-1-naphthylmethanamine (2 mmol) and CS_2 (4 mmol) were mixed in PEG-200 (1 mL). The reaction mixture was stirred at room temperature for 30 min. After completion of the reaction (monitored by TLC), reaction mixture was

extracted with 1:1 ethyl acetate/water. The ethyl acetate layer was dried over anhydrous Na_2SO_4 and the solvent was removed at reduced pressure to yield the sensor 1.

4.2 Synthesis of hydroxyl derivative (b1) from chloro derivative (b)

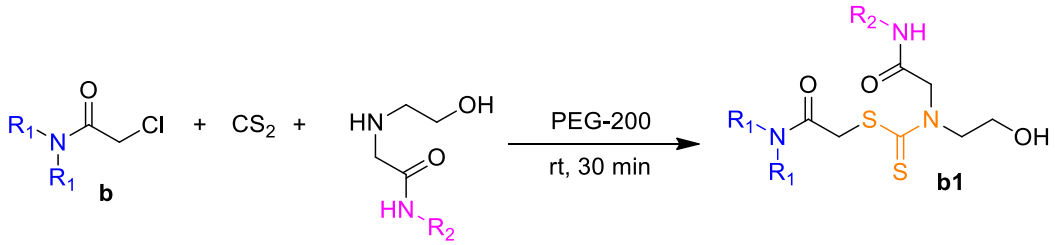

Scheme S4. Synthesis of hydroxyl derivative **b1**

Chloro terminal amide (**b**, 1 mmol), the respective monomer (2 mmol) and CS_2 (4 mmol) were mixed in PEG-200 (1 mL). The reaction mixture was stirred at room temperature for 30 min. After completion of the reaction (monitored by TLC), reaction mixture was extracted with 1:1 ethyl acetate/water. The ethyl acetate layer was dried over anhydrous Na_2SO_4 and the solvent was removed at reduced pressure and the product was used for the next step without further purification.

4.3 Synthesis of chloro derivative (c) from hydroxyl derivative (b1)

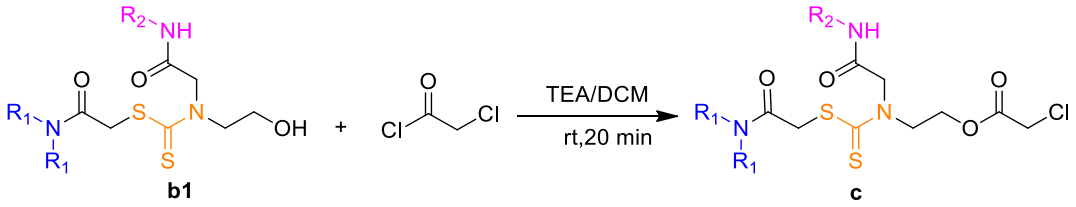

Scheme S5. Synthesis of chloro derivative **c**

The hydroxy derivative (**b1**, 1 mmol) and chloroacetyl chloride (2 mmol) was reacted in presence of triethylamine (2 mmol) base and dichloromethane as solvent at room temperature. After the reaction (monitored by TLC), the excess chloroacetyl chloride was quenched by sodium bicarbonate ($NaHCO_3$) solution. The dichloromethane was filtered through anhydrous Na_2SO_4 bed. The solvent was removed under reduced pressure. The chloro derivative (**c**) was taken directly for dithiocarbamate reaction without further purification.

4.4 Synthesis of sensor 2

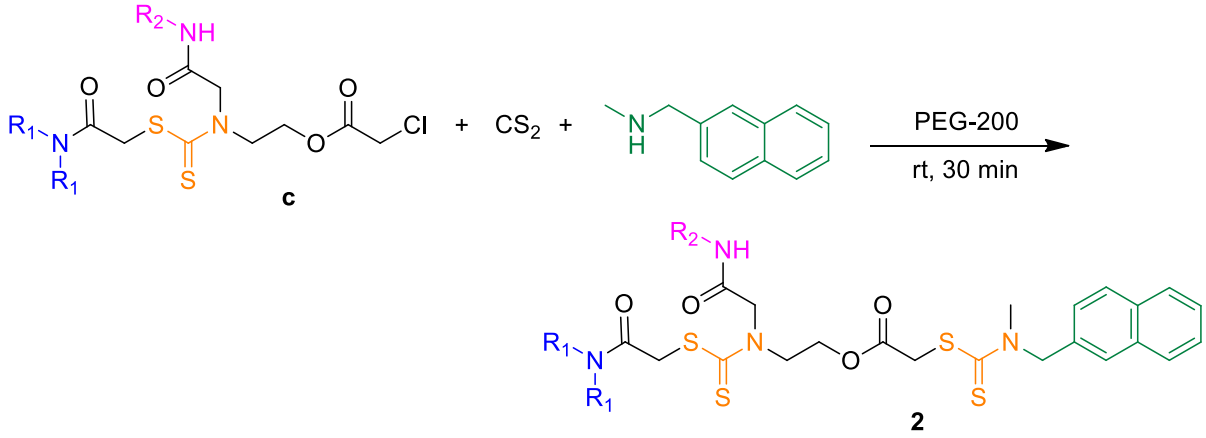

Scheme S6. Synthesis of sensor **2**

Similar procedure for the synthesis of sensor **1** was followed to synthesize **2** as well.

4.5 Synthesis of hydroxyl derivative (c1) from chloro derivative (c)

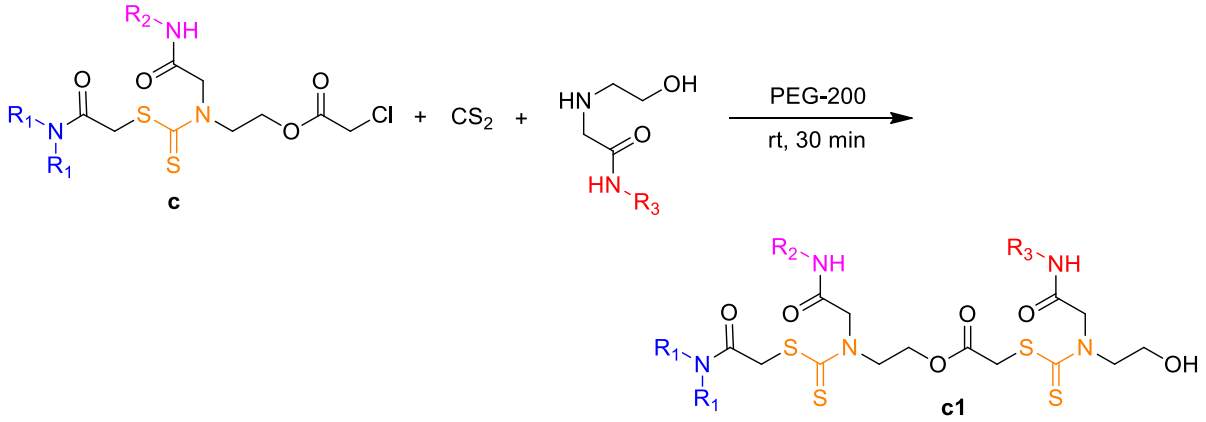

Scheme S7. Synthesis of hydroxyl derivative **c1**

Similar procedure for the synthesis of **b1** was followed to synthesize **c1**.

4.6 Synthesis of chloro derivative (d) from hydroxyl derivative (c1)

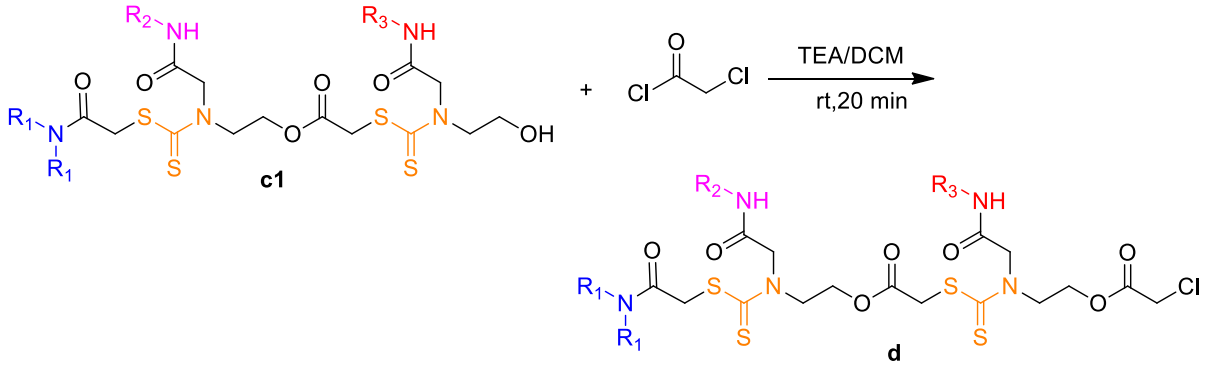

Scheme S8. Synthesis of chloro derivative **d**

Similar procedure for the synthesis of **c** was followed to synthesize **d**.

4.7 Synthesis of sensor 3

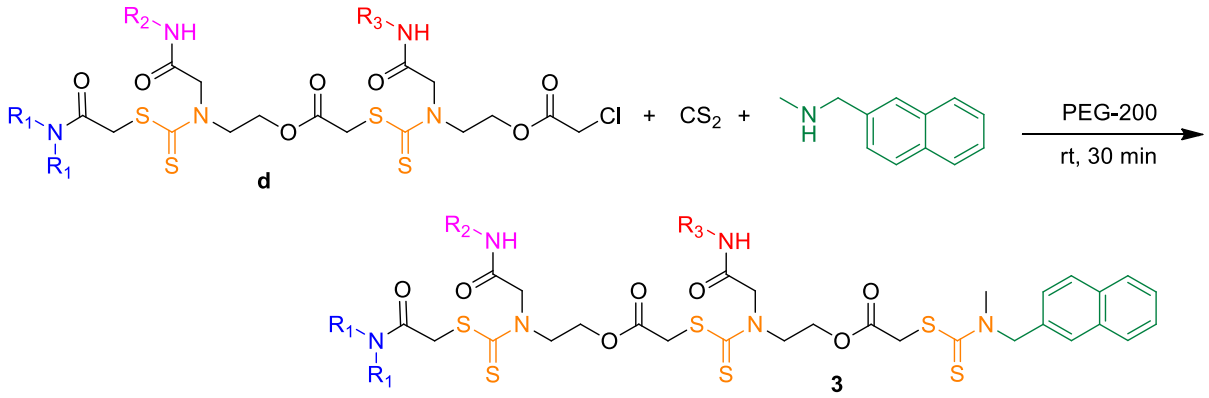

Scheme S9. Synthesis of sensor **3**

Similar procedure for the synthesis of sensor **1** and **2** was followed to synthesize **3** as well.

5. LC of the synthesized sensors

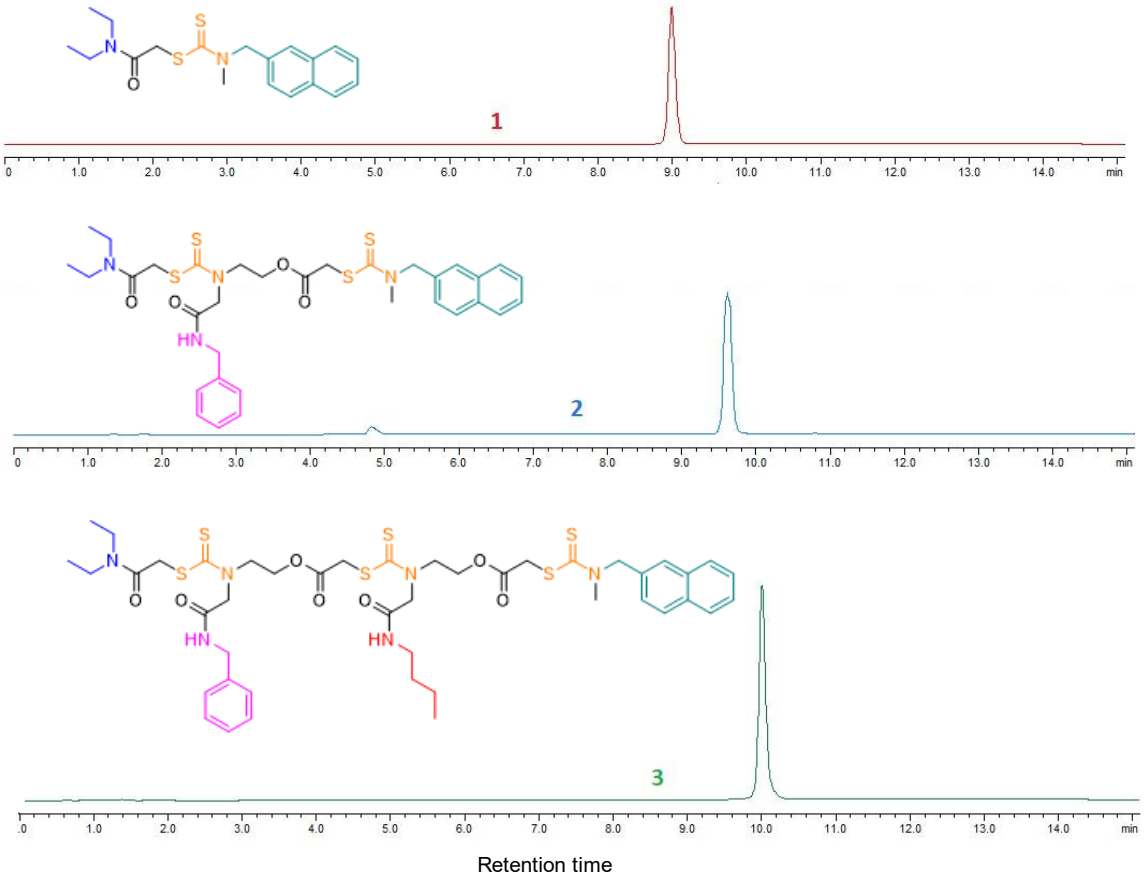

Fig S3. LC of the synthesised sensors **1**(red), **2** (blue) and **3** (green)

6. ^{1}H-NMR of the synthesised sensors

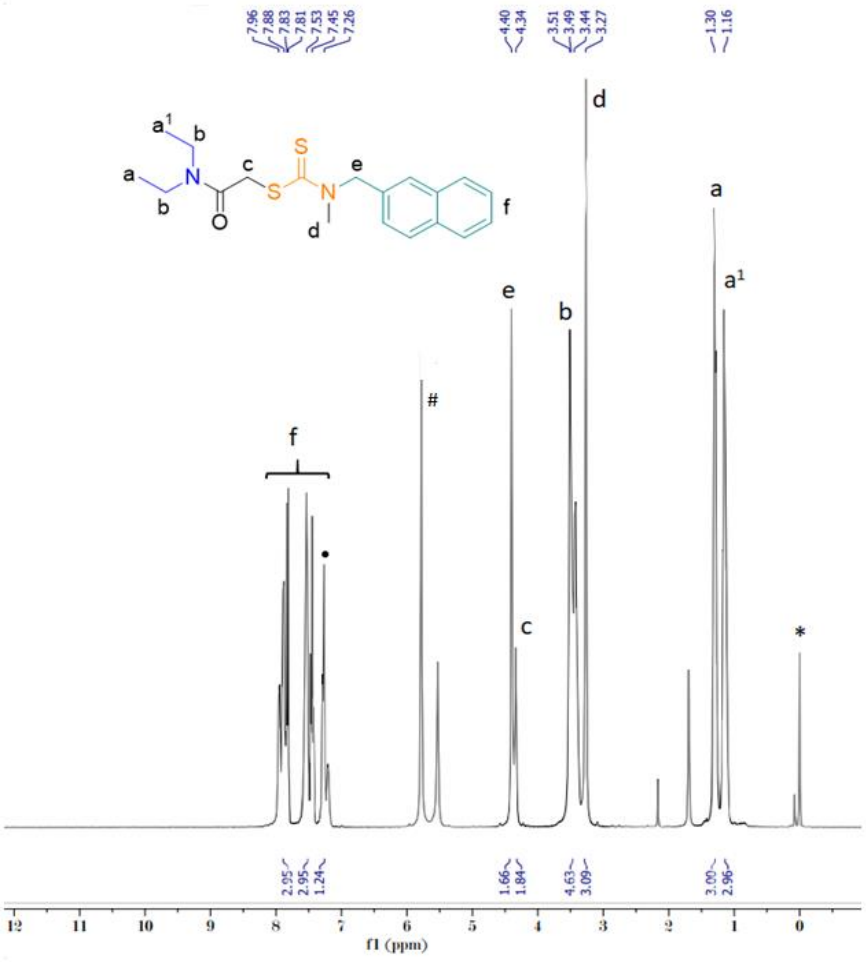

Fig S4. ^{1}H-NMR (400MHz) of sensor **1** in $CDCl_3$: δ (ppm) 1.16-1.30 (t, 6H), 3.27 (s, 3H), 3.44-3.51 (m, 4H), 4.34-4.40 (m, 4H), 7.26-7.45 (d, 2H), 7.53-7.81 (d, 3H), 7.83-7.96 (d, 3H). *, #, and • represents the residual protons of internal standard trimethyl silane, CD_2Cl_2 and $CDCl_3$ respectively.

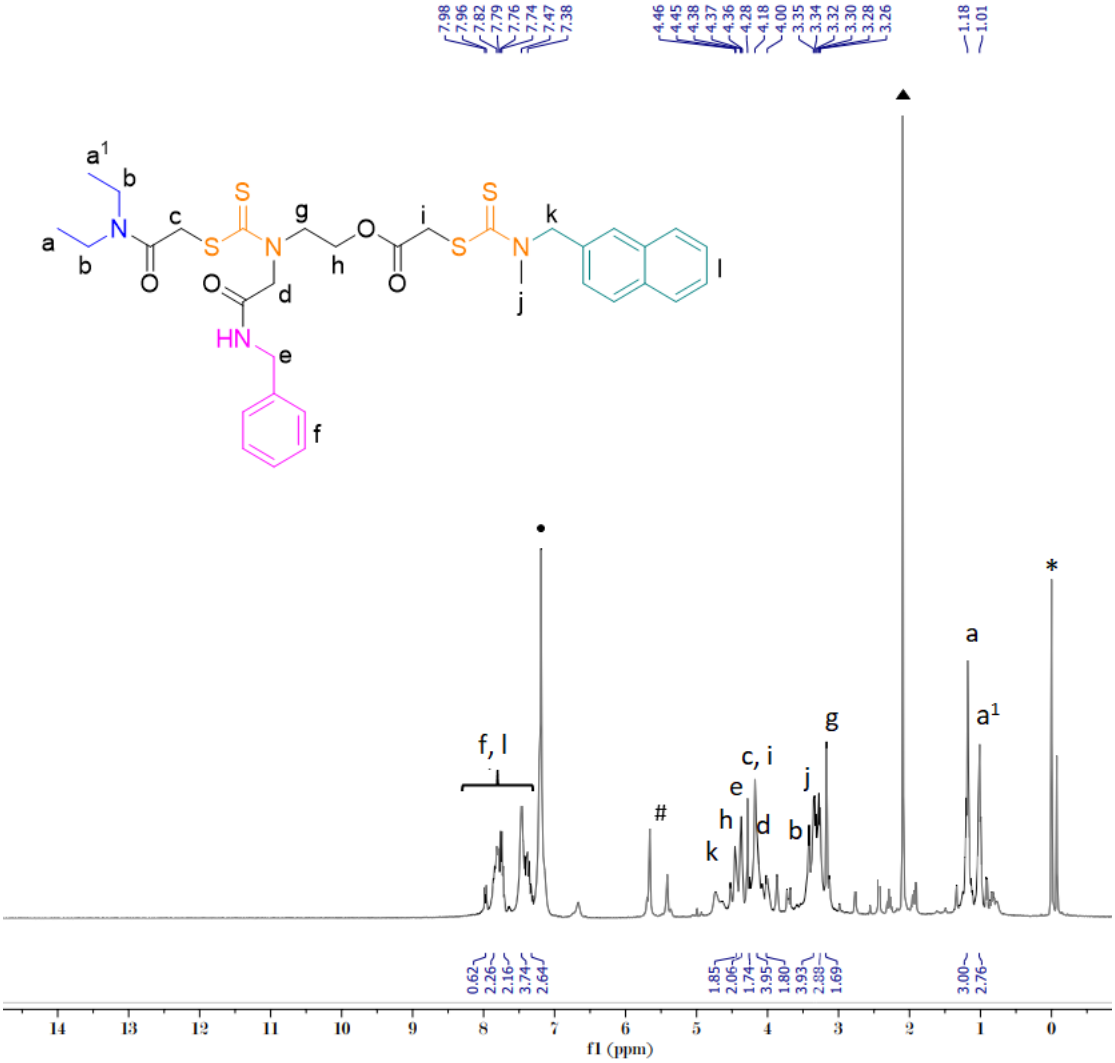

Fig S5. ^{1}H-NMR (400MHz) of sensor **2** in $CDCl_3$: δ (ppm) 1.10-1.18 (t, 6H), 3.26-3.28 (t, 2H), 3.28 (s, 3H), 3.30-3.35 (m, 4H), 4.00 (s, 2H), 4.18-4.4.28 (m, 4H), 4.36 (s, 2H), 4.37-4.46 (m, 4H), 7.38-7.47 (3H), 7.47-7.74 (4H), 7.74-7.76 (d, 2H, 8J), 7.76-7.82 (2H), 7.96-7.98 (d, 1H, 8J). *, •, # and ▲ represents the residual protons of internal standard trimethyl silane, $CDCl_3$ CD_2Cl_2 and acetone respectively.

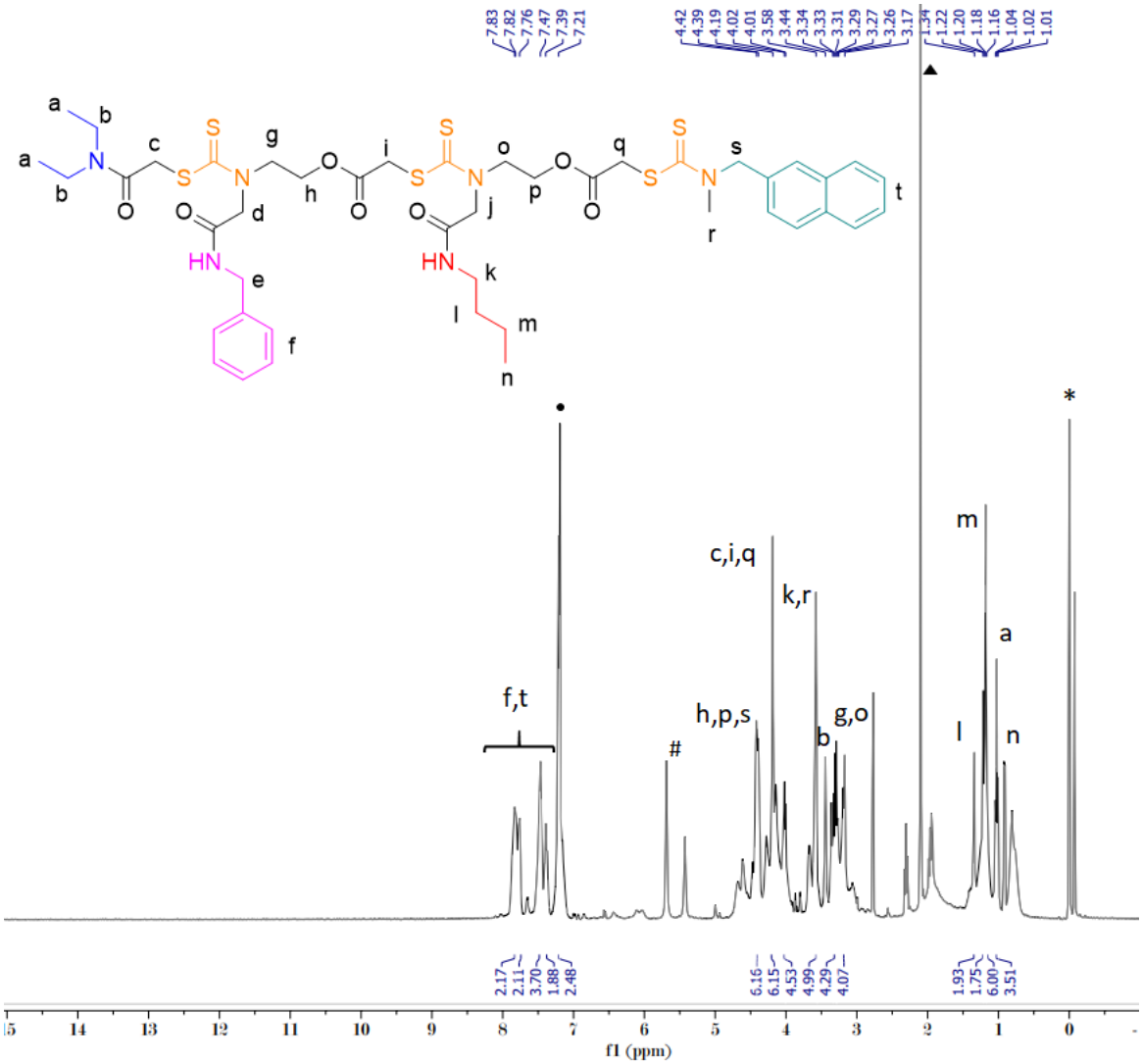

Fig S6. ^{1}H-NMR (400MHz) of sensor **3** in $CDCl_3$: δ (ppm) 1.01-1.02 (t, 3H), 1.02-1.04 (t, 6H), 1.16-1.20 (m, 2H), 1.22-1.34 (m, 2H), 3.17-3.27 (m, 4H), 3.29-3.34 (m, 4H), 3.44-3.58 (m, 5H), 4.01-4.02 (m, 4H), 4.19-4.39 (m, 6H), 4.39-4.42 (m, 6H), 7.21-7.39 (2H), 7.39-7.47(2H), 7.47-7.76 (4H), 7.76-7.82 (2H), 7.82-7.83 (2H). *, •, # and ▲ represents the residual protons of internal standard trimethyl silane, $CDCl_3$, CD_2Cl_2 and acetone respectively.

7. Fluorescence spectra of 1, 2 and 3

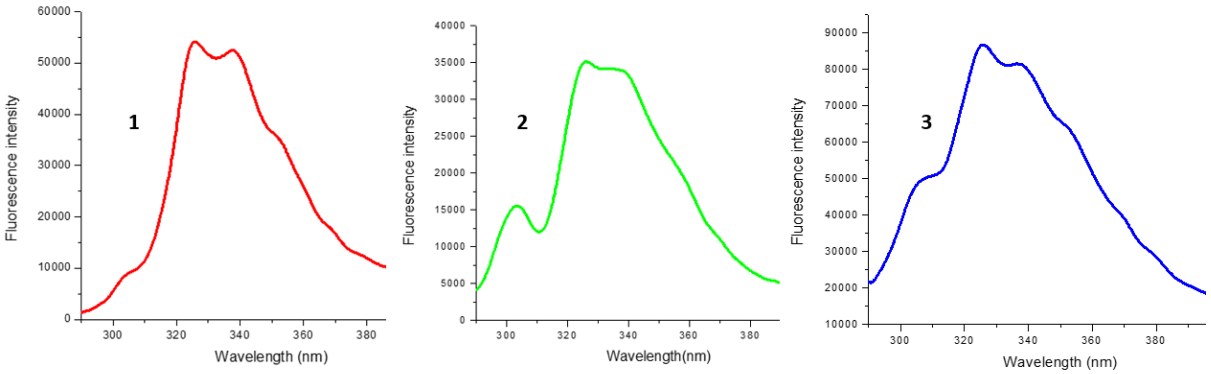

Fig S7. Fluorescence spectra of **1, 2** and **3** (10µM) in methanol at 25^0C and excitation wavelength of 278 nm.

8. Selectivity studies for sensors 2 and 3

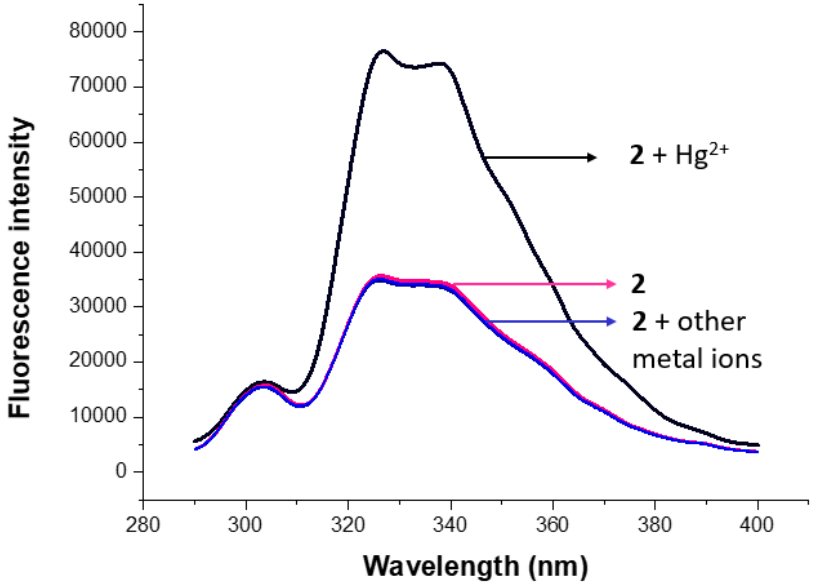

Fig S8. Fluorescence spectra of **2** (10µM) in presence of different metal ions (Al^{3+}, Zn^{2+}, Cd^{2+}, Pb^{2+}, Fe^{2+}, Fe^{3+}, Mn^{2+}, Na^{+}, Co^{2+}, Cu^{2+}, Ni^{2+} and Ca^{2+}) 20µM in methanol at 25^0C and excitation wavelength of 278 nm.

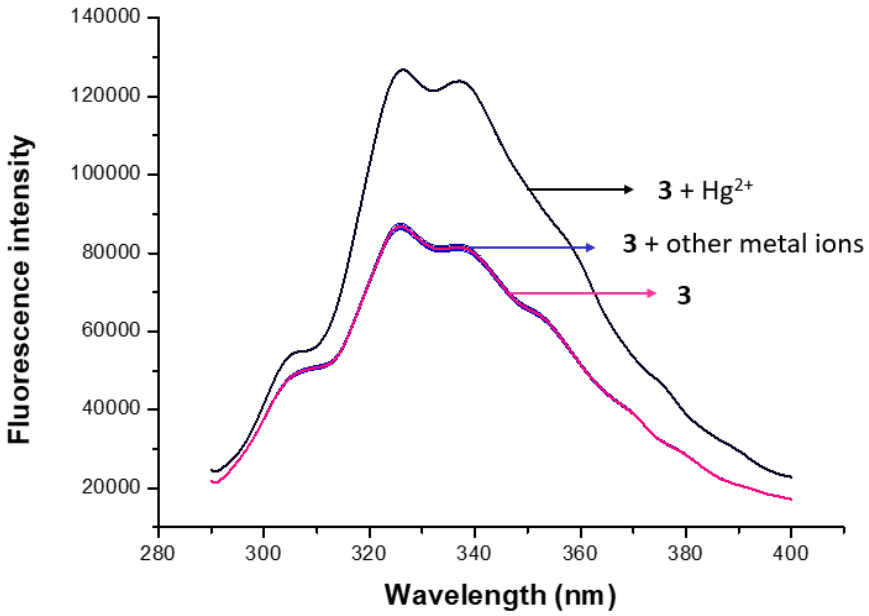

Fig S9. Fluorescence spectra of **3** (10µM) in presence of different metal ions (Al^{3+}, Zn^{2+}, Cd^{2+}, Pb^{2+}, Fe^{2+}, Fe^{3+}, Mn^{2+}, Na^{+}, Co^{2+}, Cu^{2+}, Ni^{2+} Ca^{2+}) 30µM in methanol at 25^0C and excitation wavelength of 278 nm.

Sensitivity measurement for 1 and 2

The sensor **1** efficiently detected the presence of Hg^{2+} ions in the range of 1- 10nM but not in any lower Hg^{2+} ions concentrations which is depicted in the figure below (FigS17). Here sensor **1** is titrated with Hg^{2+} in the range of 10-100pM. Similarly, in the case of sensor **2**, detection of Hg^{2+} ions were not observed beyond the concentration range of 10pM (Fig S11).

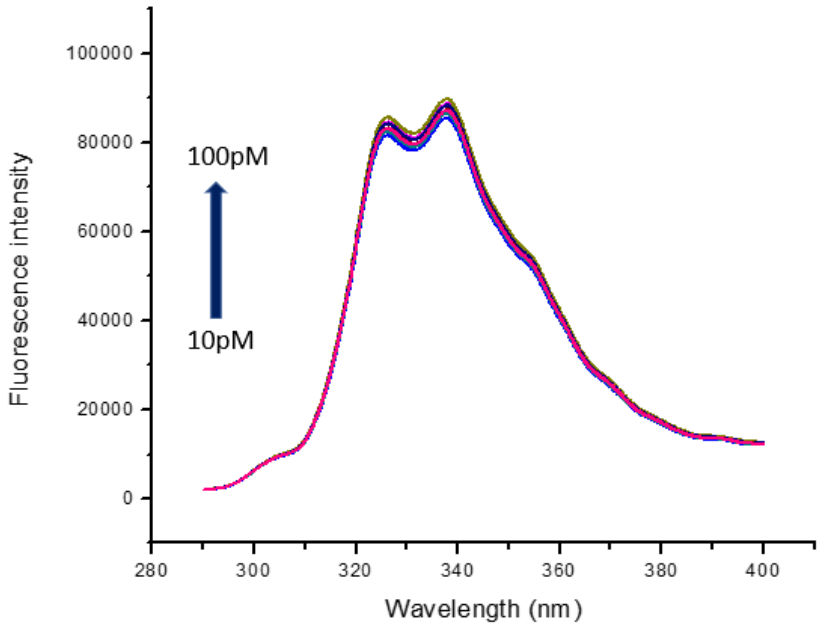

Fig S10. Fluorescence intensity of **1** (10µM) with Hg^{2+} (10- 100pM) in methanol at 25^0C and excitation wavelength of 278 nm.

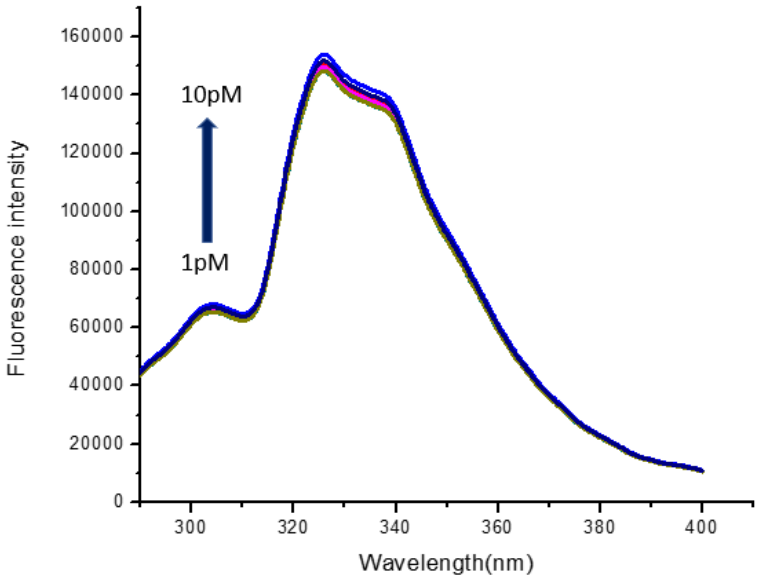

Fig S11. Fluorescence intensity of **2** (10µM) with Hg^{2+} (1- 10pM) in methanol at 25^0C and excitation wavelength of 278 nm.

9. Fluorescence titration for LOD calculation

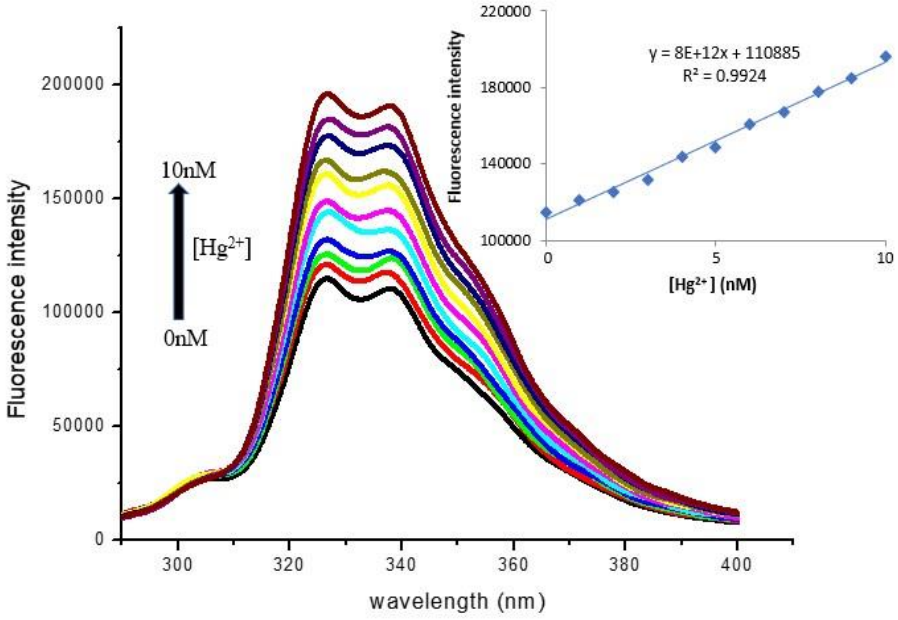

Fig S12. Fluorescence intensity of **1** (10µM) with Hg^{2+} (0- 10nM) in methanol at 25^0C and excitation wavelength of 278 nm, Inset: Hg^{2+} titration profile at 326 nm.

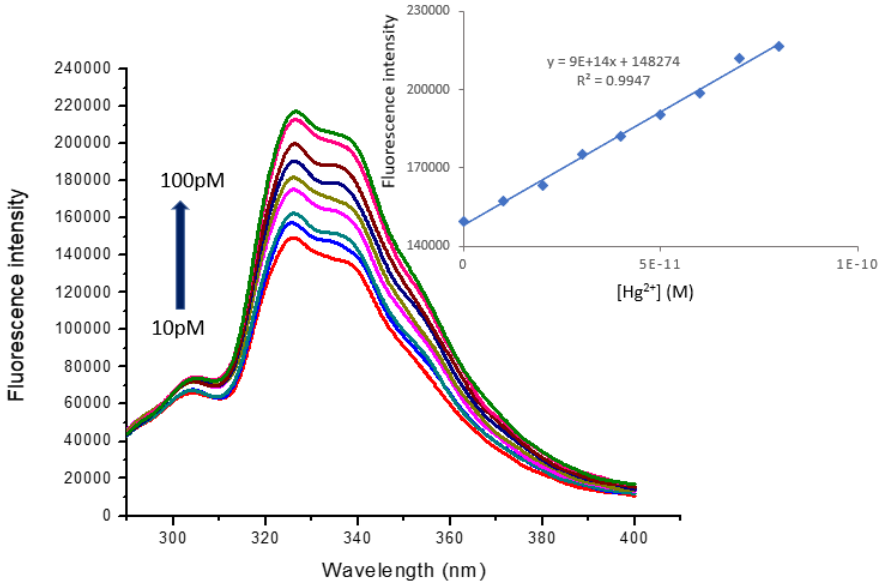

Fig S13. Fluorescence intensity of **2** (10µM) with Hg^{2+} (10- 100pM) in methanol at 25^0C and excitation wavelength of 278 nm, Inset: Hg^{2+} titration profile at 326 nm.

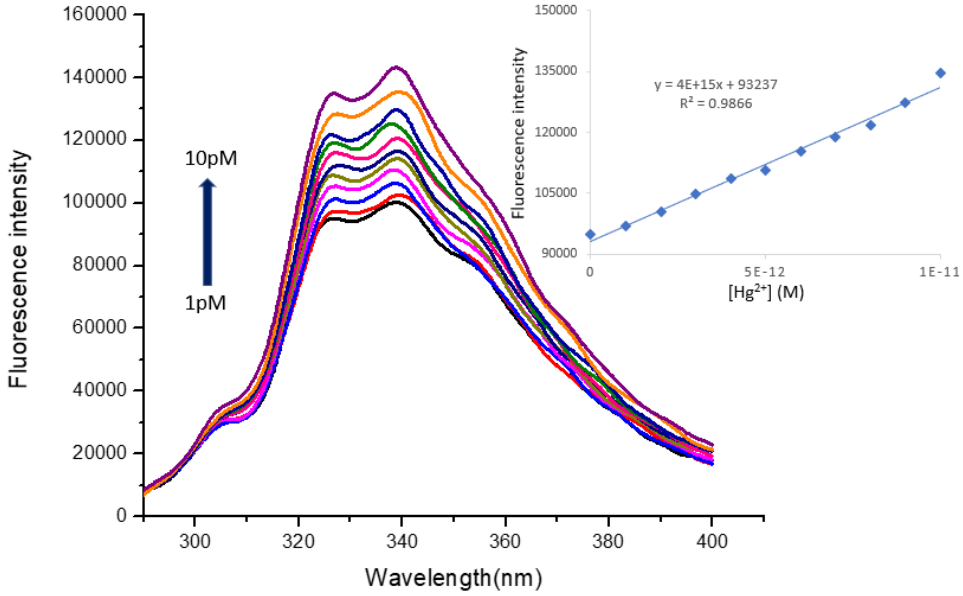

Fig S14. Fluorescence intensity of **3** (10µM) with Hg^{2+} (1- 10pM) in methanol at 25^0C and excitation wavelength of 278 nm, Inset: Hg^{2+} titration profile at 326 nm

10. Benesi- Hildebrand Plot for determination of Binding Constant

The following Benesi-Hildebrand equation was employed to determine the binding constants of the sensor-Hg^{2+} complex using fluorescent enhancement data.

$$\frac{1}{Fx - Fo} = \frac{1}{F\alpha - Fo} + \frac{1}{K[Hg]} * \frac{1}{F\alpha - Fo}$$

Where F_o, F_x, and F_α are the fluorescence intensities of the sensor in the absence of Hg^{2+} at a given concentration and concentration for complete interaction.

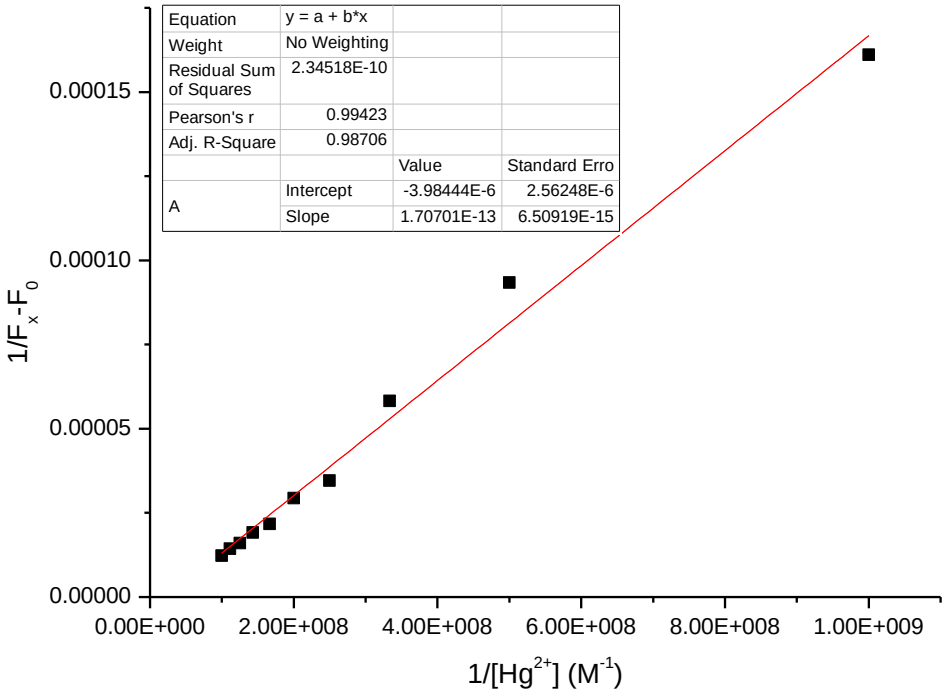

Fig S15. Benesi-Hildebrand plot for **1** + Hg^{2+}

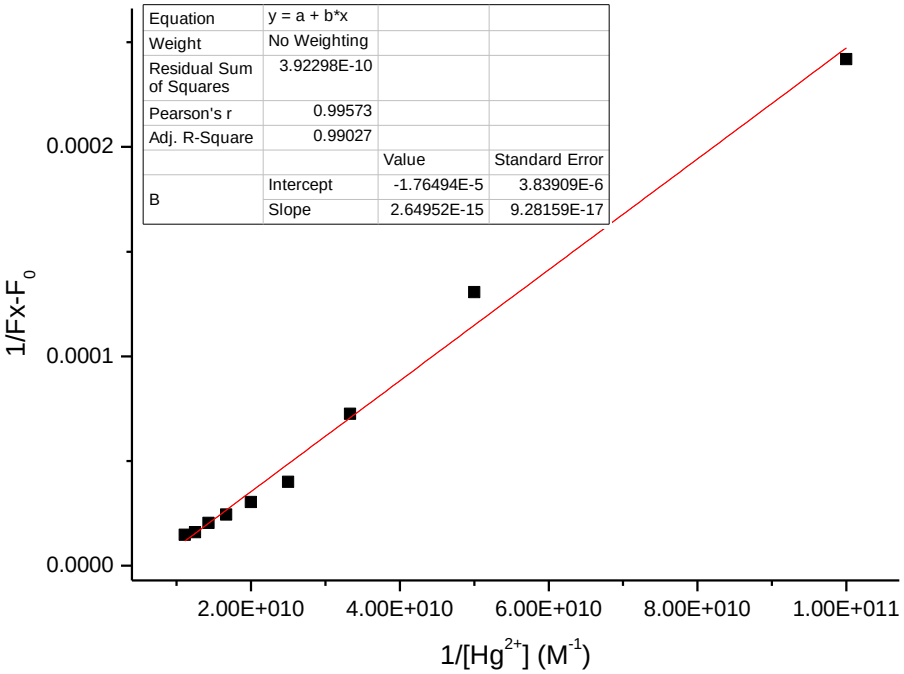

Fig S16. Benesi-Hildebrand plot for **2** + Hg^{2+}

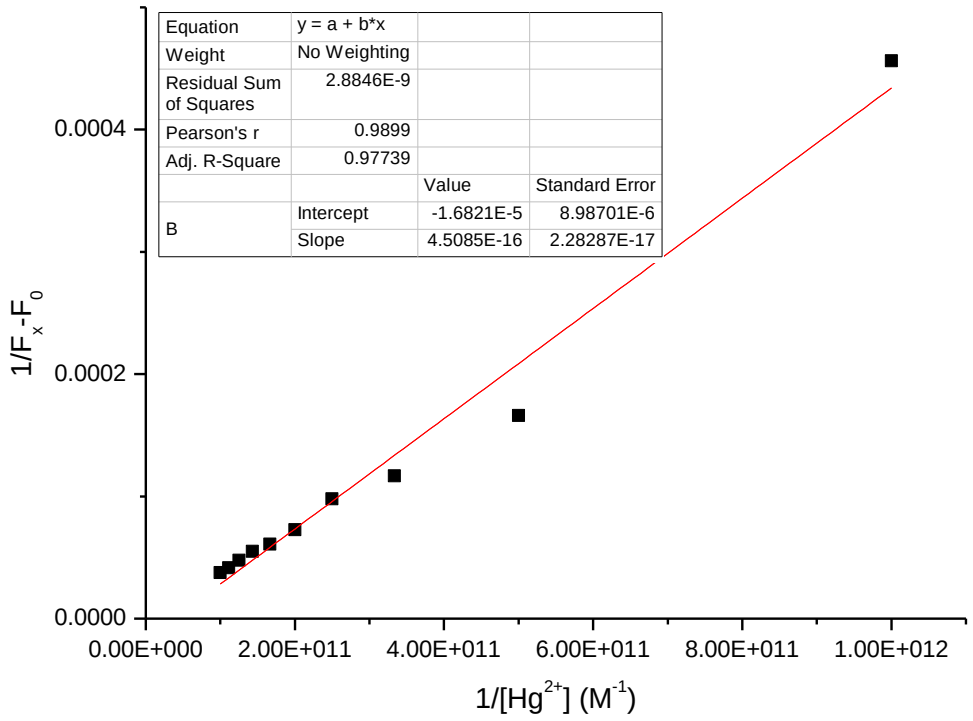

Fig S17. Benesi-Hildebrand plot for **3** + Hg^{2+}

11. Hg^{2+} induced precipitation

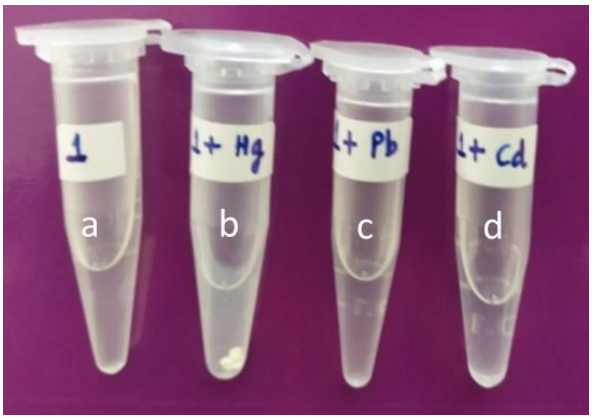

Fig S18. Photograph from left to right (a) sensor **1** (20mM), (b) **1**+Hg^{2+} (20mM), (c) **1** +Pb^{2+} (20mM), (d) **1** +Cd^{2+} (20mM) in methanol

12. Hg^{2+} induced precipitation- Characterisation by SEM (Scanning Electron Microscopy)

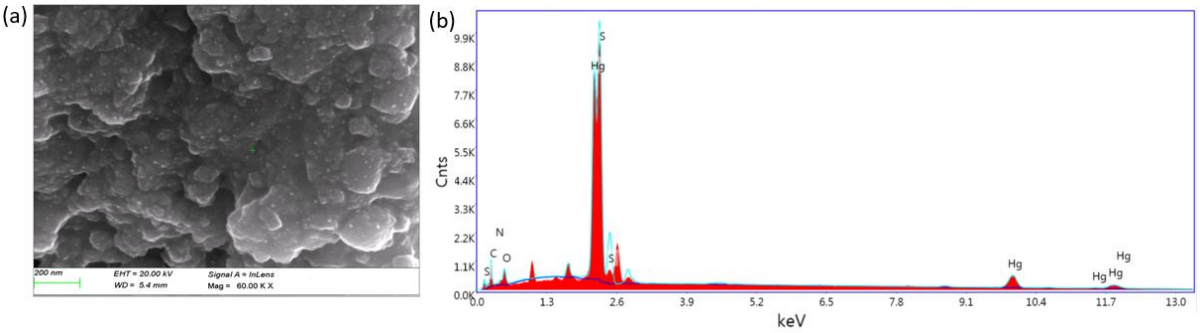

Fig S19 (a) SEM image of **1**+ Hg^{2+} (1mM) and (b) EDAX pattern of **1**+ Hg^{2+} (1mM)

Sensor **1** have two sulfur atoms which coordinates with one Hg^{2+} ion. Hence the ratio of Hg: S is 0.5. This is same as the ratio obtained from EDAX data (34.11/65.8 = 0.51) which supports the composition of **1** + Hg^{2+}.

Table S1. The atomic percentages of S and Hg in **1**+ Hg^{2+} from EDAX

Element	Atomic %
S	65.89
Hg	34.11

13. Reversibility test

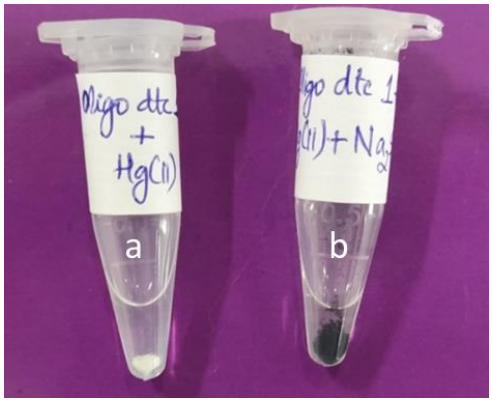

Fig S20. Photograph from left to right (a) sensor **1** (20mM) + Hg^{2+} (20mM), (b) **1** (20mM) + Hg^{2+} (20mM) +Na_2S (20mM).

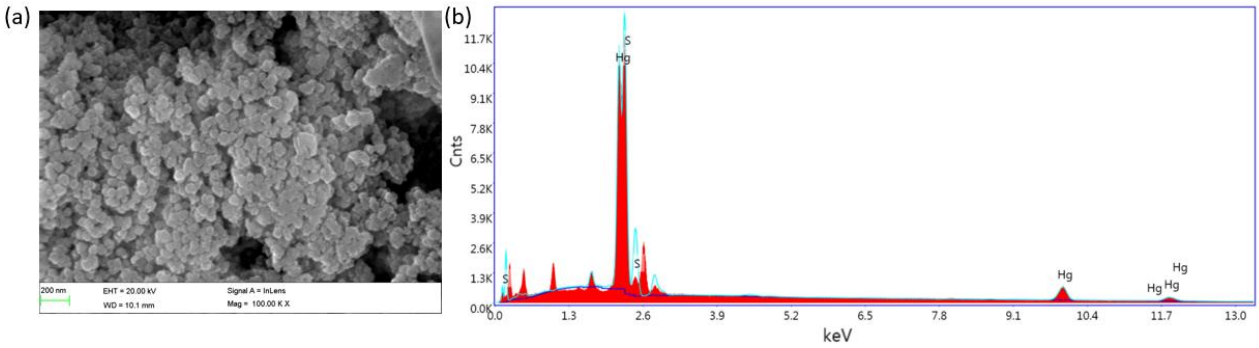

Fig S21. (a) SEM image of **1**+ Hg^{2+} + Na_2S (1mM) and (b) EDAX of **1**+ Hg^{2+} + Na_2S (2mM)

After adding Na_2S to the solution containing **1**+ Hg^{2+}, the black precipitate obtained was characterised by SEM-EDAX. The data shows the presence of Hg and S only and the ratio of Hg: S is close to 1. This shows that Hg^{2+} ions present in the solution are being precipitated as stable HgS (mercury sulphide).

Table S2. the atomic percentages of S and Hg in **1**+ Hg^{2+} + Na_2S from EDAX

Element	Atomic %
S	56.07
Hg	49.93

14. ICP-MS Data

Table S3. The concentration of Hg^{2+} in the supernatant before and after precipitation obtained from ICP-MS data

Concentration of Hg^{2+} before precipitation	Concentration of Hg^{2+} after precipitation
1.08mg/ml	0.047mg/ml

The percentage of Hg^{2+} ions present in the supernatant after precipitation= (0.047/1.08) * 100 = 4.3%

Therefore, removal efficiency = 95.7%

15. Synthesis of water-soluble sensor

To synthesise a sensor that is completely water soluble, we have designed a strategy as shown in scheme 1. Here, boc- protected ethane 1, 2 diamine (**a**, 1 mmol), was reacted with chloroacetyl chloride (2 mmol) in presence of triethylamine (2 mmol) as base and DCM to obtain the chloroacetylated product, **b**. The obtained product, **b** (1 mmol) was then treated with CS_2 (4 mmol) and the fluorophore, N-methyl-1-naphthylmethanamine (2 mmol) in PEG to form **c** with one DTC unit. This was then deprotected using 6M HCl to get the sensor denoted as **1***.

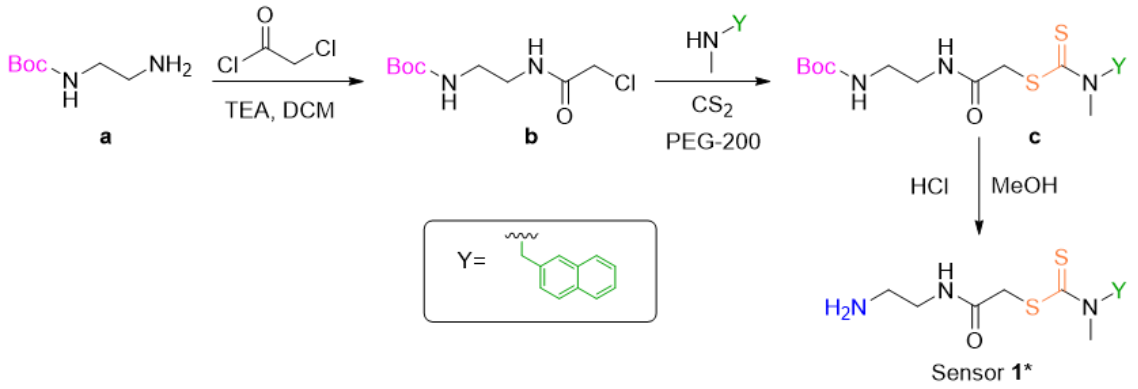

Scheme S10: Scheme for the synthesis of sensor **1***

The characterisation of the synthesised sensor **1*** was performed by LCMS and ^1H NMR is shown in Fig S22-S23.

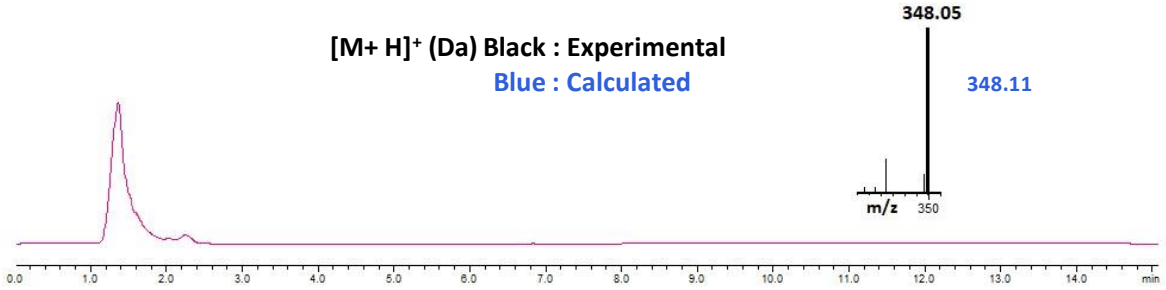

Fig S22: The LC chromatogram and characterisation by mass Spectrometry (MS) for sensor **1***. The experimental and calculated $[M+H]^+$ values are indicated.

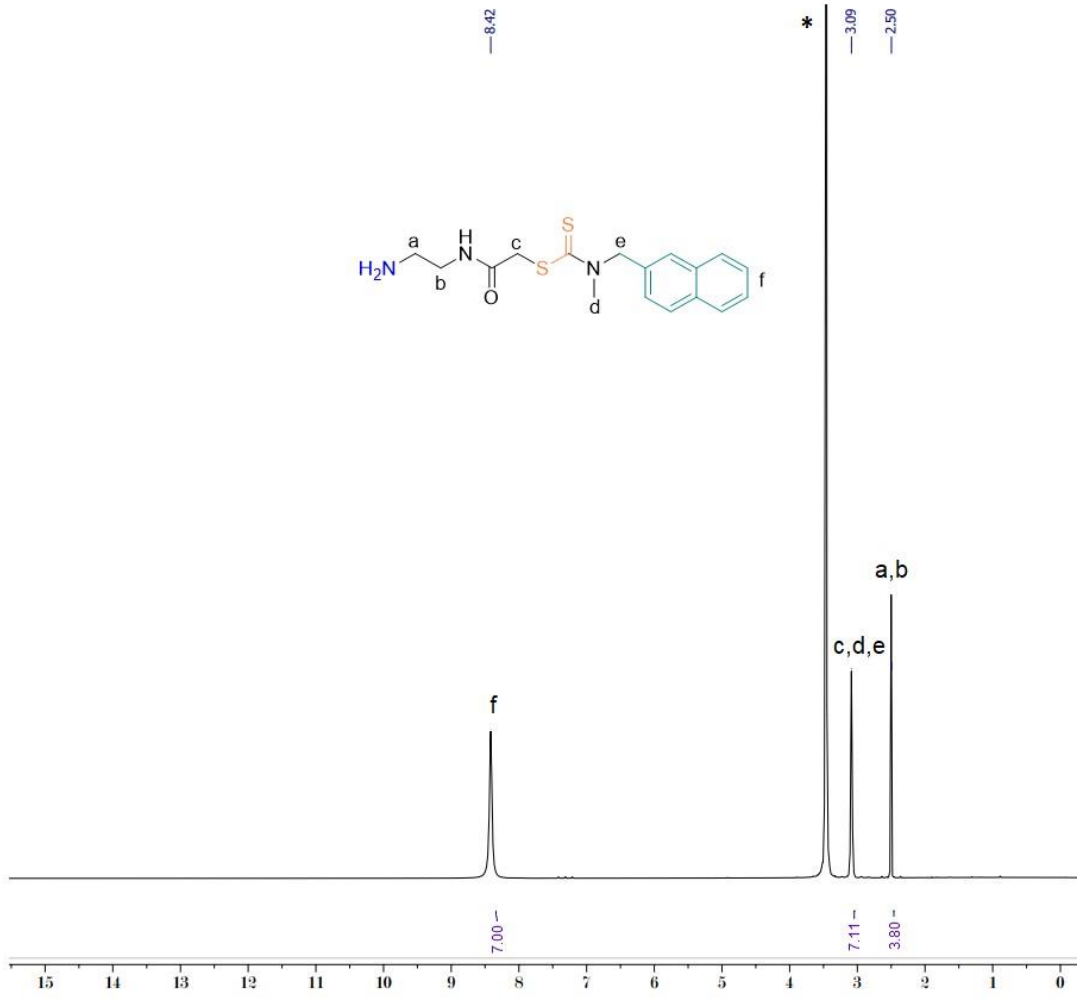

Fig S23: ^{1}H-NMR (500MHz) of sensor **1*** in DMSO: δ (ppm) 2.50 (4H), 3.09 (7H), 8.42 (7H), * represents the residual protons of H_2O.

The sensor, **1***, was completely soluble in water and the fluorescence studies were performed in 100% water. From the titration of **1*** (100µM) with 1- 10µM of Hg^{2+} (Fig S24) an LOD of 2.9 x 10^{-7}M was obtained.

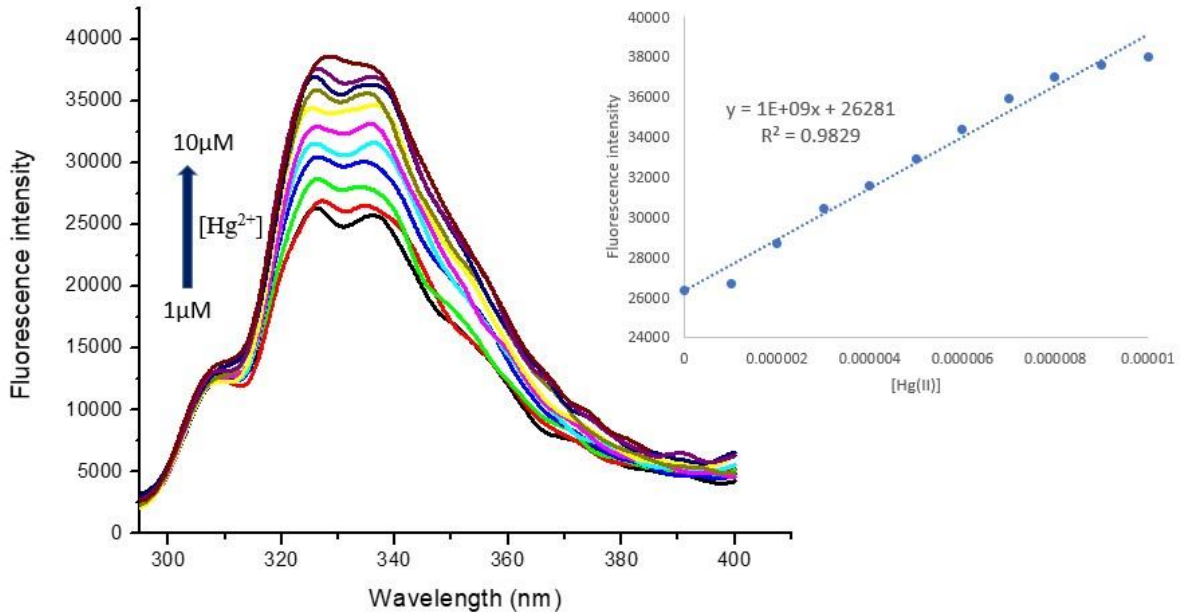

Fig S24: Fluorescence titration of **1*** (10µM) with Hg^{2+} (1 – 10µM in water at 25^0C and excitation wavelength of 278 nm. Inset: Hg^{2+} titration profile at 326 nm.

Therefore, the new sensor, 1* proves to be promising candidate for sensing environmental samples also. Increasing the number of receptor units (DTC) to this new sensor can give better sensitivity results in water. Thus, this strategy of a modular platform can be attuned to cater the requirements of the user.